УДК 539.4: 517.958:539.3; 621.9.06

SPATIAL STRESS-STRAIN STATE OF THE BORING BAR FRONT-END STRUCTURE OF HEAVY-DUTY HORIZONTAL BORING LATHE DEPENDING ON THE BORING RADIUS

[1]**Sherbakov S.S.,** PhD, DSc, [2]**Wu S.,** PhD, [2]**Shao J.,** PhD, [1]**Nasan Aleh A.**

[1]Belarusian State University, Minsk, Belarus
[2]Harbin University of Science and Technology, Harbin, China

Introduction. The object of the research is the multi-element tribo-fatigue boring bar front-end structure which is one of the most critical components of heavy-duty horizontal boring lathe (see Figure 1a). Contact interaction with friction between its various elements and a non-contact bending are implemented in this system.

The aim of the work was to determine stress-strain state of the system and to find out the position of its bodies for minimizing stress while increasing the boring radius.

FEM based computer simulation of the boring bar front-end structure was made considering its contact interactions during the boring process and non-contact deformation occurring due to the bending of the cutter.

Problem statement. Suppose that $\mathbf{r}^k$ is the position of the particular configuration of the k-th body in space for calculated system, shown on Figure 1b, 1c. For them the following relations that determine the mechanical state of the particle of the body (the elementary volume) are carried out: the continuity equation, the equation of equilibrium of the body's particles, dependency between displacements and strains, and Hooke's law [1, 2].

Boundary conditions of the first type for the surface S_u of the lower body of analyzed system on the axes Y on the Figure 1b, where displacements $\overline{u}_i^{k*}\left(\mathbf{r}^k\right)$ are set, are added to the equations that determine the mechanical state:

$$u_i^k = \overline{u}_i^{k*}\left(\mathbf{r}^k\right), i = x, y, z\,, \tag{1}$$

and the second type for all other elements of the system, on the surface S_σ of which the effort distributions $\overline{p}_i$, represented on Figures 1b and 1c are set:

$$\sigma_{ij}^k \alpha_j^k = \overline{p}_i^k\left(\overline{\mathbf{F}}_N, \mathbf{r}^k\right), \tag{2}$$

where α_j^k – direction cosines.

Interaction of n deformable bodies of the system can be described with the help of the contact boundary conditions, defined by the next relations:

$$\overline{\mathbf{u}}_l\big|_{S_u^{(lm)}} - \overline{\mathbf{u}}_m\big|_{S_u^{(lm)}} = \boldsymbol{\delta}_{lm}^{(u)}\left(f_{lm}, \mathbf{r}^l, \mathbf{r}^m, t\right)\Big|_{S_u^{(lm)}},, \tag{3}$$

$$\overline{\mathbf{p}}_l\Big|_{S_\sigma^{(lm)}} - \overline{\mathbf{p}}_m\Big|_{S_\sigma^{(lm)}} = \boldsymbol{\delta}_{lm}^{(\sigma)}\left(f_{lm}, \mathbf{r}^l, \mathbf{r}^m, t\right)\Big|_{S_u^{(lm)}}, \tag{4}$$

where $S^{(lm)}$ – contact surface for bodies l and m, $S_\sigma^{(lm)} \subset S^{(lm)}$, $S_u^{(lm)} \subset S^{(lm)}$, $\overline{\mathbf{p}}_k = \left\{\overline{p}_1^k, \overline{p}_2^k, \overline{p}_3^k\right\} = \left\{p_n^k, p_{\tau 1}^k, p_{\tau 2}^k\right\}$ and $\overline{\mathbf{u}}_k = \left\{\overline{u}_1^k, \overline{u}_2^k, \overline{u}_3^k\right\}$ – vectors of forces and displacements on the surface of k-th body, $p_n^k, p_{\tau 1}^k, p_{\tau 2}^k$ – normal and tangential components of the vector forces, $\boldsymbol{\delta}_{lm}^{(u)} = \{\delta_{lm}^{(n,u)}, \delta_{lm}^{(\tau 1,u)}, \delta_{lm}^{(\tau 2,u)}\}$, $\boldsymbol{\delta}_{lm}^{(\sigma)} = \{\delta_{lm}^{(n,\sigma)}, \delta_{lm}^{(\tau 1,\sigma)}, \delta_{lm}^{(\tau 2,\sigma)}\}$ – vectors of displacements and forces on the contact surface, f_{lm} – friction coefficients for the corresponding pairs of bodies.

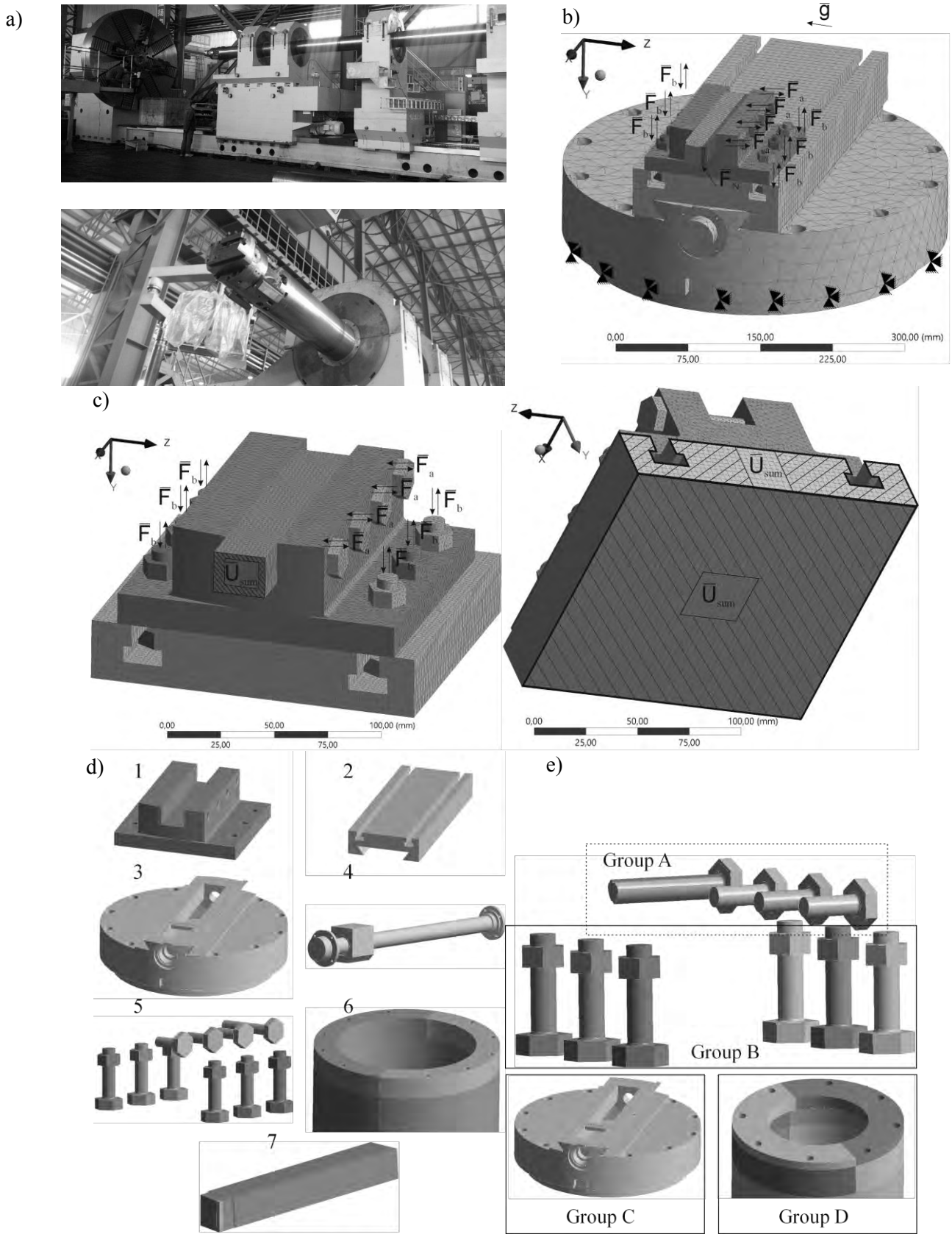

Fig. 1. Studied system: a) heavy-duty horizontal boring lathe and its front-end structure; b) finite element mesh and loading scheme for full model of the front-end structure; c) finite element mesh and loading scheme for submodeling regions of the front-end structure; d) elements of the boring bar front-end structure (1 – upper base, 2 – middle base, 3 – lower base, 4 – shaft, 5 – bolts, 6 – boring bar, 7 – cutter); e) groups of bolted connections

Finite-element models with applied boundary conditions are shown in Figures 1b-1c and the mechanical characteristics of the materials used are given in Table 1.

Friction coefficient f equals 0.18 for all contact interactions.

Boring load was defined according to the data provided by the Harbin University of Science and Technology: $\overline{F}_N$ = {-3118; 3619; -8620} N. Force $\overline{F}_N$ was applied to the three external faces of the cube of the boring part of the knife with an edge length of 4 mm.

Table 1 – Mechanical characteristics

Material	Poisson's Ratio, ν	Young's modulus, E, GPa	Yield strength, $\sigma_т$, MPa	Strength limit, σ_c, MPa
Steel 18ХГТ, (for bolts)	0.3	211	885	980
Steel 18ХГТ	0.3	211	730	980

For calculation of tightening force of bolt joints the methodology described in [3] was used. Considering a metric thread and the beginning of the plasticity in the bolts rods, tighten force in bolt joints, represented on Figures 1b, 1c, 1e, are shown in the Table 2.

Table 2 – Bolts pretension

Screw type	Group	Bolt pretension, N
M8x1 – 6g	A	F_a = 24949.5
M10x1 – 6g	B	F_b = 43048.7
M14x1,5 – 6g	C	F_c = 82341.3
M24x2 – 6g	D	F_d = 264903

Let us denote generalized coordinate q_1 according to the notation given on Figure 1d which represents the displacement of the upper support relative to the middle support in the guides of the middle support.

Let us also denote generalized coordinate q_2 that represents the displacement of the middle support on the shaft relative to the lower support fixed on the boring bar.

Positive direction of generalized coordinates q_1 and q_2 is defined as a movement in the direction of increasing the boring radius. Origin for q_1 and q_2 is the position of the system provided by the Harbin University of Science and Technology and presented in Figures 1b-1c. In this case, the parameterization of the calculation grid can be specified in the form $Q_{i,j}$, where i takes the calculated values of q_1, and j are the discrete values of q_2, respectively. Thus, in Table 3, a correspondence was made between the codification of the calculations $Q_{i,j}$ and the boring radii.

It can be seen from Table 3 that exactly the same boring radii can be achieved by different displacements of the upper and middle supports.

All calculations were performed in the finite element simulation program ANSYS Workbench considering gravitational force field in a static formulation.

In accordance with well-proven technology provided in [4] calculations for all models were divided into two phases: the first step took into account the tightening of bolted joints, during the second one the boring load was added.

At the second step the distribution of forces and displacements produced by the tightening of bolted joints were applied as the boundary conditions.

For a more accurate finite element evaluation of stress-strain state of the front-end system of the boring bar the submodeling of the front end system (cutter, upper base and a piece of middle base) was made. It was carried out by transferring displacements which were derived from calculations of the full models to the submodeled faces shown in Figure 1c as well

as the application of remaining boundary conditions in this domain. After that new boundary problem was solved.

Table 3 – Boring radii for calculations $Q_{i,j}$ (mm)

		j			
i	$Q_{i,j}$	1, q_2 = 0 mm	2, q_2 = 21.65 m m	3, q_2 = 94.15 m m	4, q_2 = 111.65 m m
	1, q_1 = -18.756 mm	218.24	239.89	312.39	329.89
	2, q_1 = 0 mm	236.996	258.646	331.146	348.646
	3, q_1 = 18.756 mm	255.752	277.402	349.902	367.402

Stress state. Figure 2 represents distributions of equivalent stress σ_{eqv} for the calculations which correspond to the extreme values of the generalized coordinates q_1 and q_2: $Q_{1,1}$, $Q_{3,1}$, $Q_{1,4}$, $Q_{3,4}$.

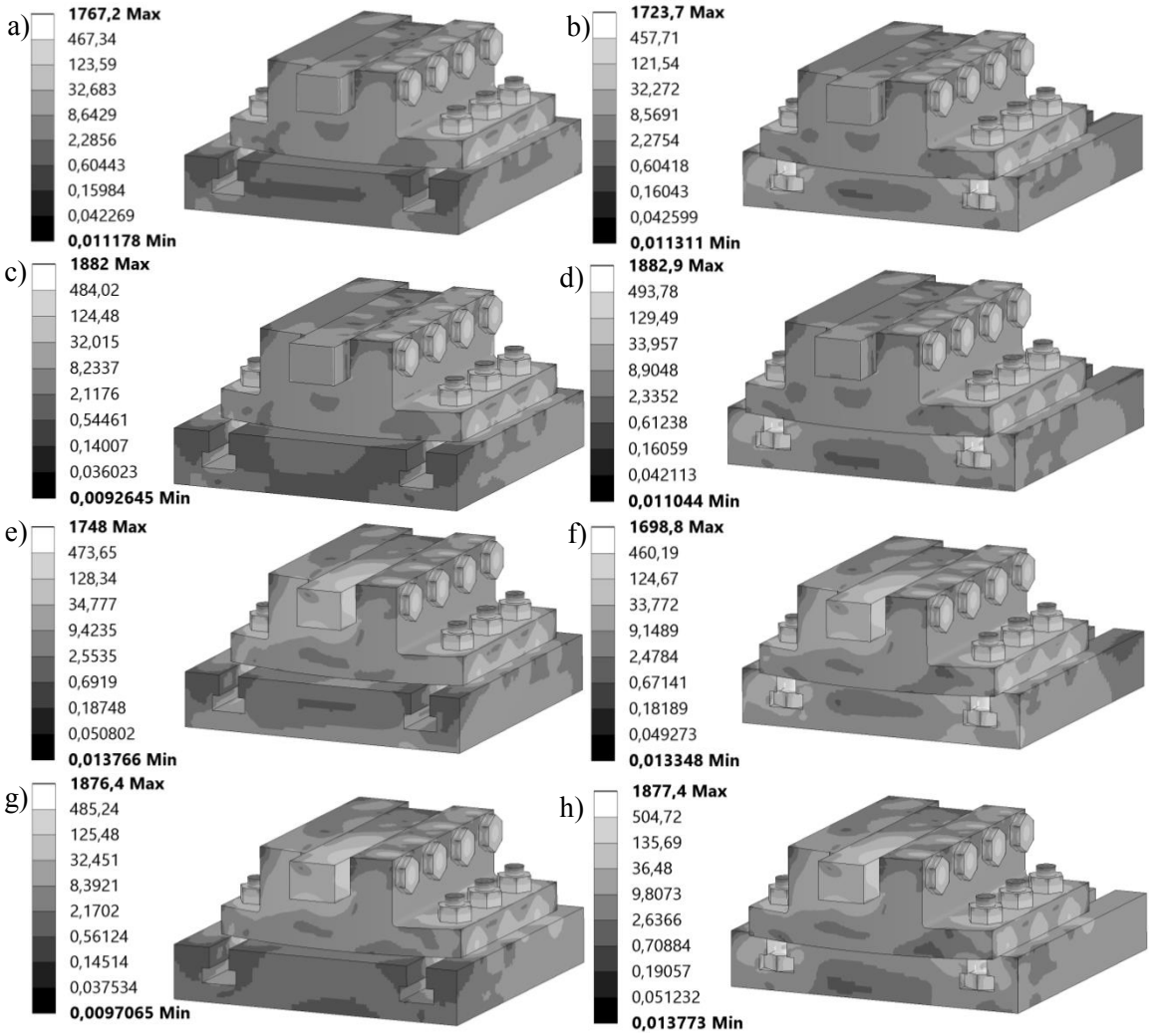

Fig. 2. Distributions of equivalent stress σ_{eqv} after tightening the bolted joints in the submodels, MPa: a) $Q_{1,1}$; b) $Q_{3,1}$; c) $Q_{1,4}$; d) $Q_{3,4}$ and distributions of equivalent stress σ_{eqv} during boring process in the submodels, MPa: e) $Q_{1,1}$; f) $Q_{3,1}$; g) $Q_{1,4}$; h) $Q_{3,4}$;

According to Figures 2-3 depending on the different radii of boring it is seen that in the system during submodeling after tightening the bolted joints the maximum value of the equivalent stress σ_{eqv} appears to be the least in the calculation $Q_{1,2}$, amounting to 1702.7 MPa and σ_{eqv} increases by 10.69 % to the highest value of 1884.8 MPa in the calculation $Q_{2,4}$.

In the submodeled system during the boring process, the maximum value of the equivalent stress σ_{eqv} appears to be the least in the calculation $Q_{1,2}$, amounting to 1645.1 MPa and σ_{eqv} increases by 14.18 %, to the highest value of 1878.5 MPa in the calculation $Q_{2,4}$.

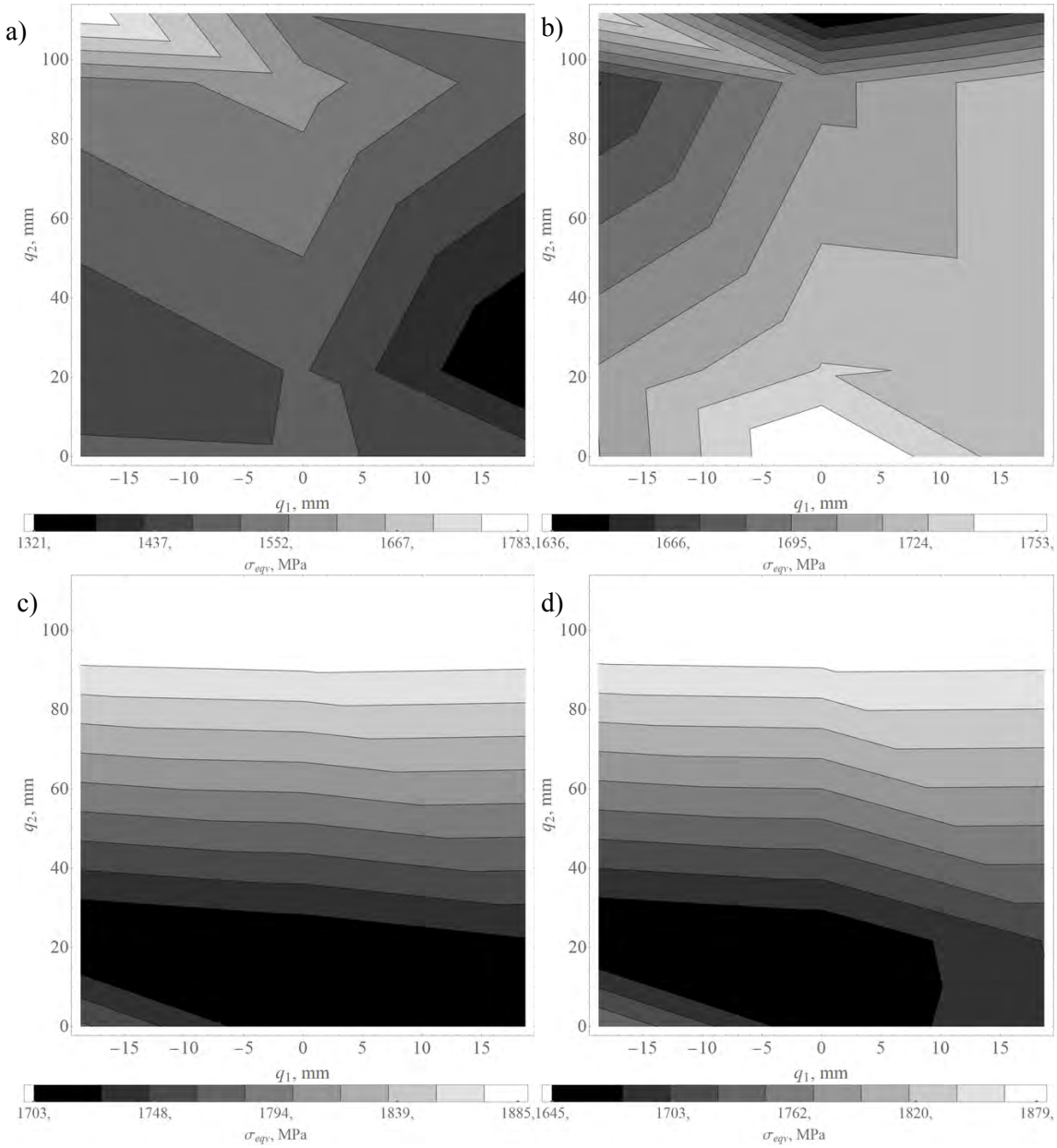

Fig. 3. Maximum equivalent stress σ_{eqv} in the whole system depending on the value of the generalized coordinates q_1 and q_2 (positions of the bases), MPa: a) after tightening the bolted joint in the full models; b) during boring process in full models; c) after tightening the bolted joint in submodels; d) during boring process in submodels

After tightening the bolted joints in the full model in the system the maximum value of the equivalent stress σ_{eqv} appears to be the least in the calculation $Q_{3,2}$, amounting to 1321.1 MPa and σ_{eqv} increases by 34.95 % to the highest value of 1782.8 MPa in the calculation $Q_{1,4}$. The minimum and maximum values of the maximum equivalent stress in full model decrease

by 22.41 % and 5.41 % as compared with the lowest and highest values in the submodels respectively.

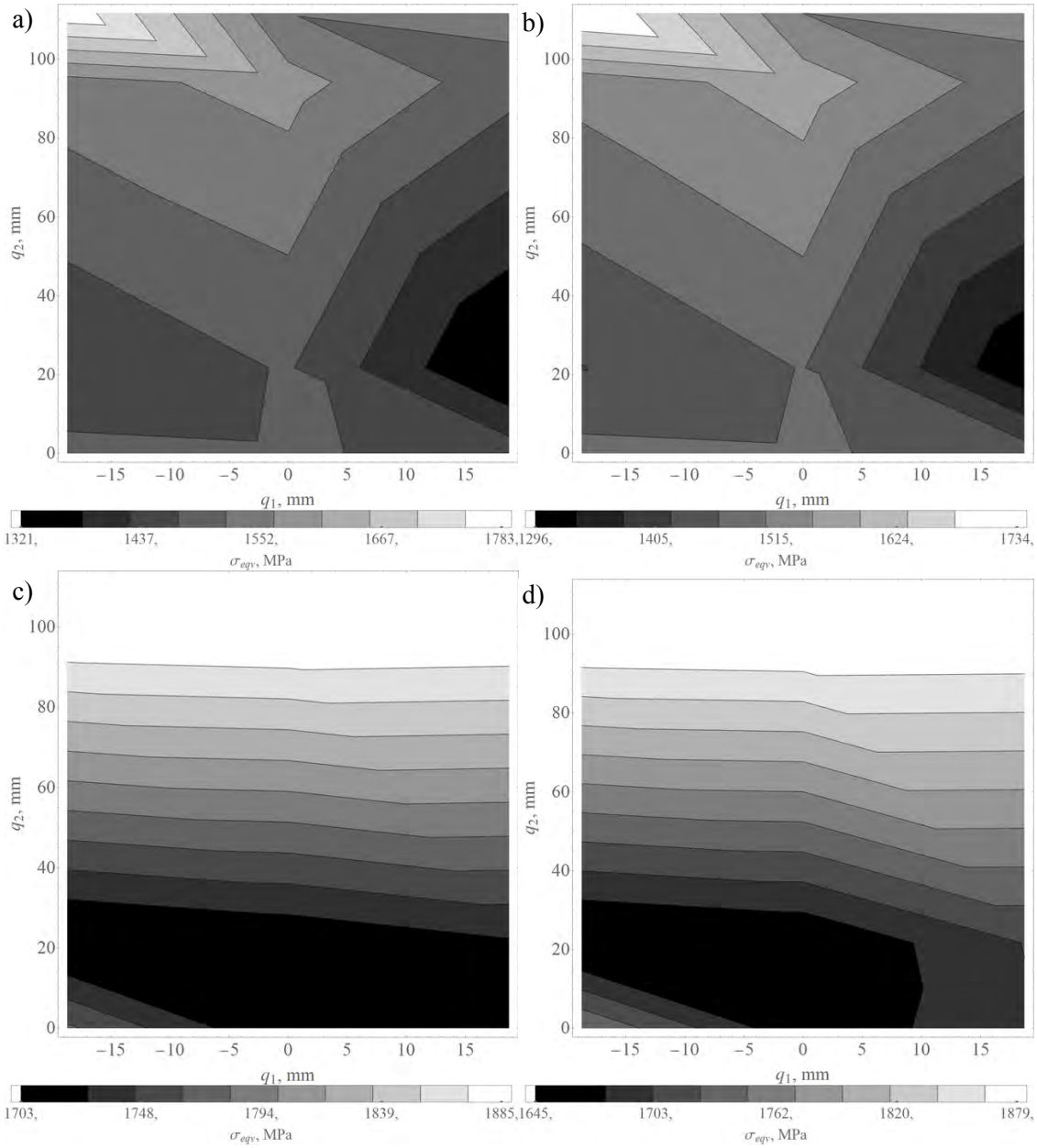

Fig. 4. Maximum equivalent stress σ_{eqv} in the bolted joints of group A and B depending on the value of the generalized coordinates q_1 and q_2 (positions of the bases), MPa: a) after tightening the bolted joint in full models; b) during boring process in full models; c) after tightening the bolted joint in submodels; d) during boring process in submodels

During the boring process in the full model in the system, the maximum value of the equivalent stress σ_{eqv} appears to be the least in the calculation $Q_{2,4}$, amounting to 1636.3 MPa and σ_{eqv} increases by 7.14 % to the highest value of 1753.2 MPa in the calculation $Q_{2,1}$. The minimum and maximum values of the maximum equivalent stress in full model decrease by 0.53 % and 6.67 % as compared to the lowest and highest values in the submodels, respectively.

As it's shown on Figure 4, after tightening the bolted joints in the full model in the bolts of both group A and B, the maximum value of the equivalent stress σ_{eqv} appears to be the least in the calculation $Q_{3,2}$, amounting to 1321.1 MPa and σ_{eqv} increases by 34.95 % to the highest value of 1782.8 MPa in the calculation $Q_{1,4}$. The minimum and maximum values of the max-

imum equivalent stress in full model decrease by 22.41 % and 5.41 % as compared with the lowest and highest values in the submodels, respectively.

During the boring process in the full model in the bolts of both group A and B, the maximum value of the equivalent stress σ_{eqv} appears to be the least in the calculation $Q_{3,2}$, amounting to 1295.8 MPa and σ_{eqv} increases by 33.78 % to the highest value of 1733.5 MPa in the calculation $Q_{1,4}$. The minimum and maximum values of the maximum equivalent stress in full model decrease by 21.23 % and 7.72 % as compared to the lowest and highest values in the submodels, respectively.

Conclusion. During this study 24 mechanical and mathematical models allowing description of the three-dimensional stress-strain state of the boring bar front-end structure of heavy-duty horizontal boring lathe depending on the boring radius were developed. The effect of the bolts tightening on the upper base was investigated.

The use of submodeling made possible the research of the nature of the changes in the investigated distributions in more detail and indirectly confirmed the convergence of the solutions.

In general, it should be noted that the tightening forces of the bolted joints of groups A and B are extreme and contribute significantly to the stress-strain state of the elastic elements of the front-end structure of heavy-duty horizontal boring lathe in comparison to the impact of boring process.

The obtained results indicate that in order to minimize von-Mises stress of the most loaded bodies of the system with increasing boring radius it is better to move the middle base (increase q_2) than the upper one. Moreover, it is advisable to push the upper base as much as possible in the direction of decreasing the boring radius (decrease q_1).

Further, it is recommended to carry out additional studies of this model by making analysis focused not on local characteristics of damageability (components of stress tensor), but on integral ones such as dangerous volumes. Also it is reasonable to adjust the tightening values of bolted joints within the analysis of damageability reduction.

And it is also advisable to vary the basic sizes of bolts of groups A and B in order to determine the least damageability at an acceptable price and manufacturability of these elements.

This work was supported by National special project for international scientific and technological cooperation of the People's Republic of China (2012DFR70840).

REFERENCES

1. *Sosnovskiy, L.A. Mechanothermodynamics / L.A. Sosnovskiy, S.S. Sherbakov // – Springer, 2016. – 155 p.*
2. *Sosnovskiy, L.A. Methods and main results of Tribo-Fatigue tests / L.A. Sosnovskiy, A.V. Bogdanovich, O.M. Yelovoy, S.A. Tyurin, V.V. Komissarov, S.S. Sherbakov // International Journal of Fatigue. –2014. –Vol. 66. –pp.207-219.*
3. *Birger, I.A. Threaded and flanged joints / I.A. Birger, G.B. Iosilevich / – M.: Mashinostroenie, 1990, – 368 p. (in Russian).*
4. *Sherbakov, S.S. Spatial stress-strain state of boring bar front-end structure of heavy-duty horizontal boring lathe / S.S. Sherbakov, W. Shi, Sh. Junpeng, A. Nasan // Mechanics of Machines, Mechanisms and Materials, 2017. №3 (40) P. 102 – 108.*